Towards Matter-Antimatter Balance at RHIC
Antiparticle-to-Particle Ratios measured with BRAHMS

D. Ouerdane for the BRAHMS collaboration
Niels Bohr Institute, University of Copenhagen, Denmark

I. G. Bearden[7], D. Beavis[1], C. Besliu[10], Y. Blyakhman[6], B. Budick[6], H. Bøggild[7], C. Chasman[1], C. H. Christensen[7], P. Christiansen[7], J. Cibor[3], R. Debbe[1], E. Enger[12], J. J. Gaardhøje[7], K. Hagel[8], O. Hansen[7], A. Holm[7], A. K. Holme[12], H. Ito[11], E. Jakobsen[7], A. Jipa[10], J. I. Jørdre[9], F. Jundt[2], C. E. Jørgensen[7], R. Karabowicz[4], T. Keutgen[8], E. J. Kim[1], T. Kozik[4], T. M. Larsen[12], J. H. Lee[1], Y. K. Lee[5], G. Løvhøiden[12], Z. Majka[4], A. Makeev[8], B. McBreen[1], M. Mikelsen[12], M. Murray[8], J. Natowitz[8], B. S. Nielsen[7], J. Norris[11], K. Olchanski[1], J. Olness[1], D. Ouerdane[7], R. Płaneta[4], F. Rami[2], D. Röhrich[9], B. H. Samset[12], D. Sandberg[7], S. J. Sanders[11], R. A. Sheetz[1], P. Staszel[7], T. F. Thorsteinsen[9+], T. S. Tveter[12], F. Videbæk[1], R. Wada[8], A. Wieloch[4], and I. S. Zgura[10]
(BRAHMS Collaboration)

[1] Brookhaven National Laboratory, Upton,New York 11973, [2] Institut de Recherches Subatomiques and Université Louis Pasteur, Strasbourg, France, [3] Institute of Nuclear Physics, Krakow, Poland, [4] Jagiellonian University, Krakow, Poland, [5] Johns Hopkins University, Baltimore, Maryland 21218, [6] New York University, New York, New York 10003, [7] Niels Bohr Institute, University of Copenhagen, Denmark, [8] Texas A&M University, College Station,Texas 77843, [9] University of Bergen, Department of Physics, Bergen,Norway, [10] University of Bucharest,Romania, [11] University of Kansas, Lawrence, Kansas 66049, [12] University of Oslo, Department of Physics, Oslo,Norway, [+] *Deceased*

(Dated: Januray 28, 2002)

Measurements of the $\bar{p}/p$, K^-/K^+ and π^-/π^+ ratios are presented as a function of rapidity for the ^{197}Au+^{197}Au reaction at $\sqrt{s_{NN}} = 200$ GeV, the maximum energy for RHIC. The ratios indicate no dependence upon either the transverse momentum p_t or collision centrality for any particle specie. The π^-/π^+ ratio shows no dependence upon rapidity over the interval covered ($0.5 < y < 3$) while the K^-/K^+ decreases from 0.95 at $y \approx 0$ to 0.8 at $y \approx 3$. The $\bar{p}/p$ ratio is found to be 0.75 at $y \approx 0$ and drops as rapidity increases to $y \approx 3$ where a value of 0.25 has been measured. These values are the highest observed so far in heavy ion collisions and show a tendency for matter and antimatter to balance at midrapidity as the initial center of mass energy increases, although full transparency is not reached.

I. INTRODUCTION

The rapidity dependence of the antiparticle to particle ratios measured from collisions between gold nuclei is investigated for $\sqrt{s_{NN}} = 200$ GeV. These ratios are of importance in the study of matter-antimatter balance since they provide the relative abundance of antiparticles produced during the reaction and therefore give some hints about its dynamics, related to the degree of tranparency achieved, and the amount of energy used for particle production. Two collision scenarios limit the range of the baryon ratios ($\bar{p}/p$, $\bar{\Lambda}/\Lambda$, etc): the full-stopping case, where all the initial nucleons were transported from the beam rapidity to midrapidity ($y \approx 0$) [1, 2] and the full transparency scenario where the midrapidity zone was baryon-free, hence giving ratios equal to one at $y \approx 0$ [3]. The K^-/K^+ is relevant in strangeness production studies which should provide information about the quark matter created during the reaction. For many years, it has been proposed that observation of an enhancement in the strangeness production could be a signature of the formation of the Quark-Gluon-Plasma (QGP), suspected to have existed during the early stage of the collision [4]. The QGP may undergo different evolutions depending on whether or not a baryon free region is achieved.

II. THE BRAHMS EXPERIMENT

The data were collected by the BRAHMS collaboration during the 2001 Au+Au running period at the Relativistic Heavy Ion Collider (RHIC), Brookhaven National Laboratory (NY, USA). The system [5] used in the present measurements consists of two independent magnetic spectrometers that can be positioned over an angular range from 2.3^{o}to 30^o(forward spectrometer, FS) and from 30^{o}to 90^o(midrapidity spectrometer, MRS) with respect to the beam line (see Fig. 1). In addition to the spectrometers, which are used for detailed characterization of a few particles per event, there are global detectors used for measuring the overall characteristics of each collision seen by BRAHMS. These systems and their utilization are fully described in [5–7].

III. THE EVENT GLOBAL CHARACTERISTICS

A. The Collision Vertex

Since RHIC is a collider, the collisions don't occur at the same spatial location, like in fixed target experiments. Rather, the width of the collision vertex distribution depends on the beam bunch width (5–

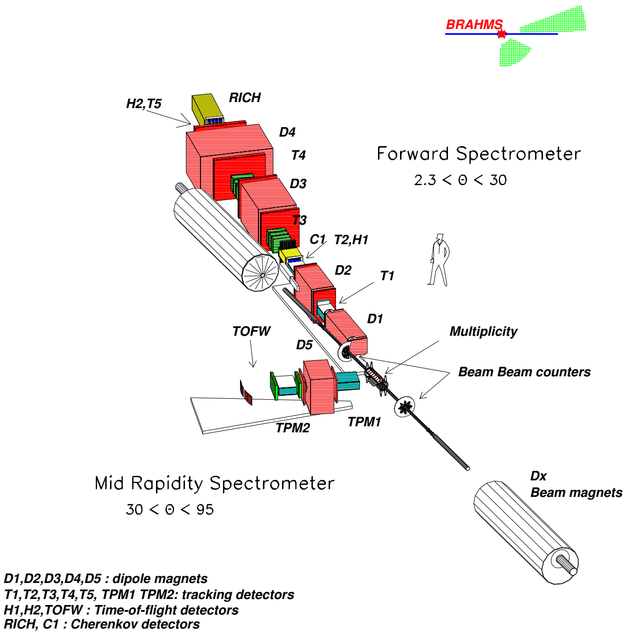

FIG. 1: The BRAHMS detector system.

15 nsec) and on the interaction diamond, which can be as wide as 1.5 meter along the beam line, as seen in the 2000 Au+Au running period. It is crucial to determine the vertex position on an event by event basis as precisely as possible since it will directly influence the quality of the particle identification (PID) (cf. section IV). The vertex position was measured by at least two independent detector systems. One of them, the beam-beam counters (BBC), was used to determine the primary vertex by calculating the time difference between the "left" and "right" arrays [5] within a resolution of 0.6 cm for the high multiplicity events (see Fig. 2).

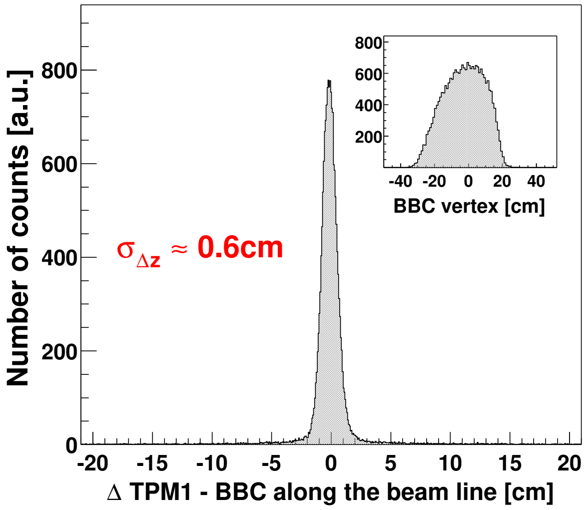

FIG. 2: Small panel: Vertex position along the beam line measured by the BBC. Large panel: difference between TPM1 track projections onto the beam line and the BBC vertex.

The other detector system used was a time projection chamber (TPC) called TPM1, located at the front of the MRS, facing directly the beam line. The track segments measured by TPM1 were projected back to the beam axis for checking their correlation with the vertex determined by the BBC (see Fig. 2, large panel). The primary vertex can be evaluated by using only valid TPM1 tracks. The resolution found is less than 0.2 cm along the beam axis but this cannot be used for all centralities due to the limited solid angle and the low average number of tracks for peripheral collisions.

B. The Collision Centrality

Another important feature of the collision is the centrality, or impact parameter (transverse distance between the original trajectories of the colliding nuclei, typically a few fermis). In ultra-relativistic heavy ion collisions, the centrality is directly related to the number of charged particles produced during the reaction: the more central the collision, the larger the charged particle multiplicity. BRAHMS has two mutiplicity detectors, the Tile Multiplicity Array (TMA) and the Silicon Multiplicity Array (SMA), (descriptions and detailed analyses can be found in [5–7]). Combined with measurements of the Zero Degree Calorimeter (ZDC), 97% of the total nuclear cross section is covered (see Fig. 3). The BBC could also be used to check the consistency of the multiplicity (see more about multiplicity results in [8]). In the present analysis, the top 25% most central events were selected.

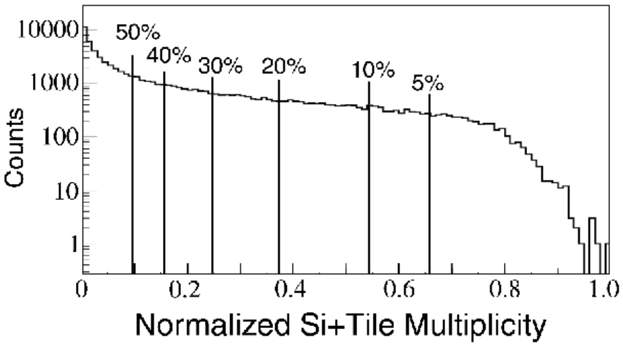

FIG. 3: Centrality determined by the TMA and SMA. The full multiplicity distribution, normalized by the highest value measured, is related to the nuclear interaction cross section covered (97% ± 2%). The different fractions of this distribution give the degree of centrality.

IV. PARTICLE IDENTIFICATION

A. MRS PID

The PID was achieved by tracking detectors and time-of-flight measurements (TOF), using the equation $\frac{1}{\beta} = \sqrt{\frac{m^2}{p^2} + 1}$ where β is the velocity of the particle, p its momentum and m its mass. The spectrometer consists of two TPC's and a dipole magnet (see Fig. 1) for flight path and momentum determination. A time–of–flight (TOF) detector of six panels positioned along a circle centered on the middle of the magnet D5 and of radius 2.4 meters is used for evaluating the TOF of the particle. Each panel contains 21 scintillator slats with PMTs at both ends. The PMT intrinsic time resolution is 65 ps while the overall TOF resolution is $\approx$ 100 ps (see Fig. 4). For the present analysis, the MRS was

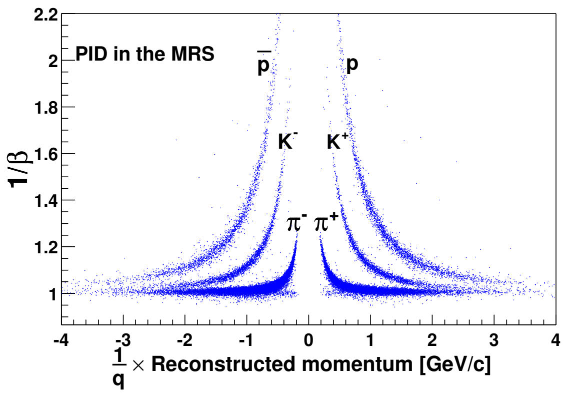

FIG. 4: Particle identification in the MRS.

operated at 90°, 60°and 45°at a field allowing the reconstruction of particle tracks above $\approx$ 0.2 GeV/c. MRS tracks were required to have a distance of closest approach to the primary vertex in the (z, y) plane of 3σ of the position resolution. In the same way, tracks were also matched with TOF hits geometrically, moreover requiring that the PMT signals were valid (software cuts). These conditions allowed a $\pi - K$ seperation up to $p \approx 2$ GeV/c whereas a $p - K$ seperation could be achieved up to $p \approx 4$ GeV/c.

B. FFS PID

The FS consists of two sections, the front forward and the back forward spectrometers (FFS and BFS). The FFS consists of two dipole magnets (D1, D2), two TPCs (T1, T2), a hodoscope (TOF1) and a Cherenkov counter (C1); the BFS is composed of two dipole magnets (D3, D4), three drift chambers (DC) named T3, T4 and T5, a hodoscope (TOF2) and a Ring Imaging Checenkov detector (see Fig. 1). In this analysis, the data were selected from the 4°, 8°and 12°settings where particle momenta ranged from $\approx$ 1 GeV/c to 20 GeV/c. Like in the MRS, tracks were required to have a distance of closest approach to the primary vertex of 3σ but in the (x, y) plane located at $z = z_{BBC}$. This choice was motivated by a larger uncertainty in the z direction, due to smaller polar angles. In Fig. 5 is plotted the PID obtained in the FFS, whereas Fig. 6 shows the performance of the BRAHMS RICH detector.

Final PID cuts are made in the MRS by selecting tracks having β^{-1} within a $\pm 2\sigma$ band of the expected β^{-1} vs. momentum for a given particle type. In the FS, the same method is used either with or without additional Cherenkov cuts depending on the momentum of the selected particles. The number of particles

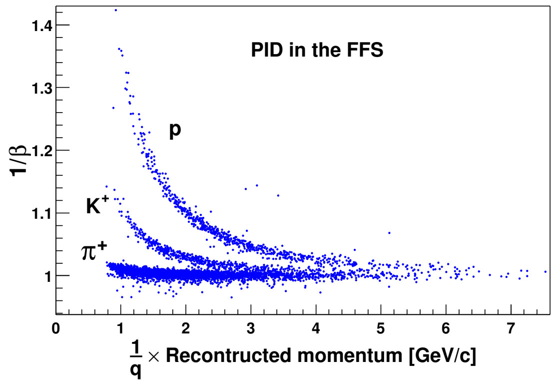

FIG. 5: Particle identification in the FFS.

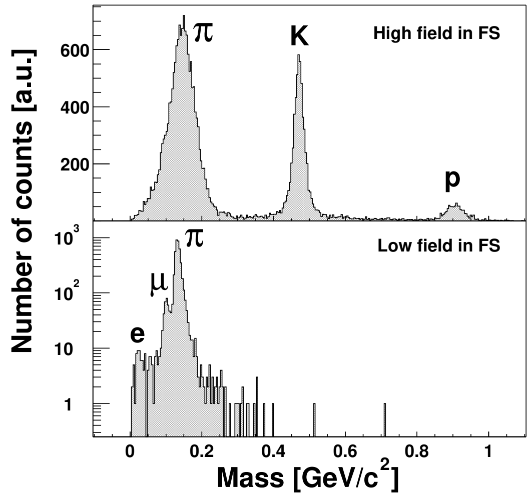

FIG. 6: Mass distribution of particles identified by the RICH. The low field data particles (bottom panel) have momenta ranging from 3 to 6 GeV/c, while the high field data particles (top panel) have momenta ranging from $\approx$ 8 GeV/c to 20 GeV/c.

measured at either field polarity was normalized to the number of collision events within the centrality cut and it was ensured that the primary vertex distributions were similar for the separate data sets within the range used in this analysis ($\pm 20cm$) in order to reduce systematic errors.

V. ANTI-PARTICLE TO PARTICLE RATIOS

The ratio measurements presented in this paper were neither corrected for weak decays nor corrected for annihilation (antiproton absorption). It was noted that background from misidentified tracks and from the tails of kaon and pion peaks had a negligible effect on the extracted ratios. In the MRS, the background contribution from slow protons, arising mainly from interaction of pions with the beam pipe is $\approx$ 10% for the lowest transverse momentum (p_t) bin. The data was corrected for this effect. In the FS, this effect is under investigation but is likely to be negligible due to the higher particle momentum range detected. Systematic errors on the measured ratios arise primarily from uncertainties in normalizations, corrections for the background of slow protons and for antiproton absorption. The dependence of the ratios with p_t was

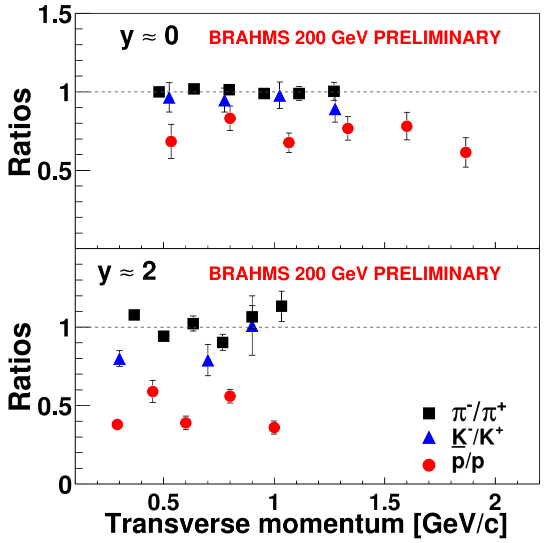

FIG. 7: Ratios versus p_t, for $y \approx 0$ (top) and $y \approx 2$ (bottom) (see text for explanations).

explored for different rapidity bins. Fig. 7 exhibits the antiparticle to particle ratios for pions, kaons and protons as a function of p_t. Only statistical errors were drawn. In the top panel, the ratios are plotted for particles at $y \approx 0$. There is no evidence of a p_t dependence in this rapidity bin within the momentum range covered. In the bottom panel, the ratios were measured at $y \approx 2$. There also seems to be no clear dependence on p_t.
In Fig. 8, it is shown that the ratios have no dependence on centrality at $y \approx 0$, though we note that only the 20% most central collisions were sampled.

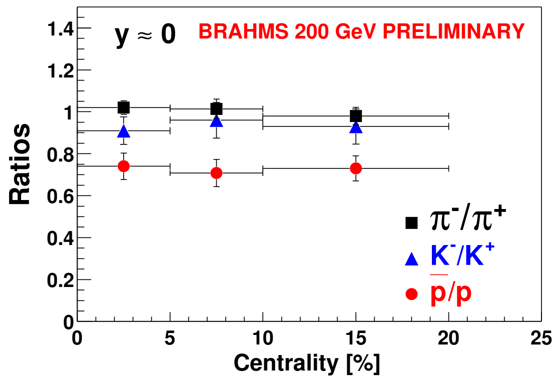

FIG. 8: Ratios versus collision centrality.

In Fig. 9 is summarized the rapidity dependence of the measured ratios, calculated for the 20 % most central collisions.
The panels depict the π^-/π^+, K^-/K^+ and $\bar{p}/p$ ratios respectively. Only statistical uncertainties are shown.

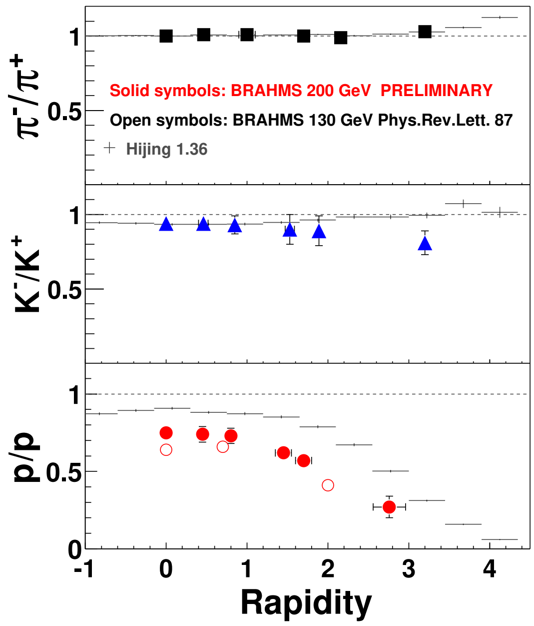

FIG. 9: Ratios as a function of rapidity. Top: π^-/π^+; middle: K^-/K^+; bottom: $\bar{p}/p$. The crosses are the corresponding ratios from HIJING [9], the open squares depicts the 130 GeV measurements [10]. Errors are statistical only. The horizontal error shows the rapidity interval covered.

It is seen that, while the pion ratio is independent of rapidity and consistent with unity, the antiproton to proton drops significantly with increasing rapidity whereas the kaon ratio decreases from 0.95 to 0.8, within the statistical errors though. The K^-/K^+ is on average very close to unity and therefore is the highest so far observed in heavy ion collisions.
The $\bar{p}/p$ ratio of 0.75 ± 0.03 (stat) ± 0.05 (syst) found at $y \approx 0$ is significantly higher than the ratio of 0.64 ± 0.04 (stat) ± 0.06 (syst) measured in Au-Au collisions at 130 GeV [10]. The ratio does not fall rapidly in the first unit of rapidity, which could imply that there is only a small degree of stopping in the collisions. These ratios were finally compared to calculations using the HIJING model [9], where the same centrality cuts as in the data analysis were applied. Hyperon decays have not been included in this calculations, but was found to affect the results by less than 4%. It can be seen that HIJING systematically overpredicts the antiproton to proton ratio over the range of rapidity covered.

Finally, in Fig. 10 is plotted the K^-/K^+ (top panel) and $\bar{p}/p$ (bottom panel) at midrapidity as a function of $\sqrt{s_{NN}}$. The initial center of mass energy dependence is very strong and indicates a systematic increase of the antiparticle production for both K^- and $\bar{p}$.

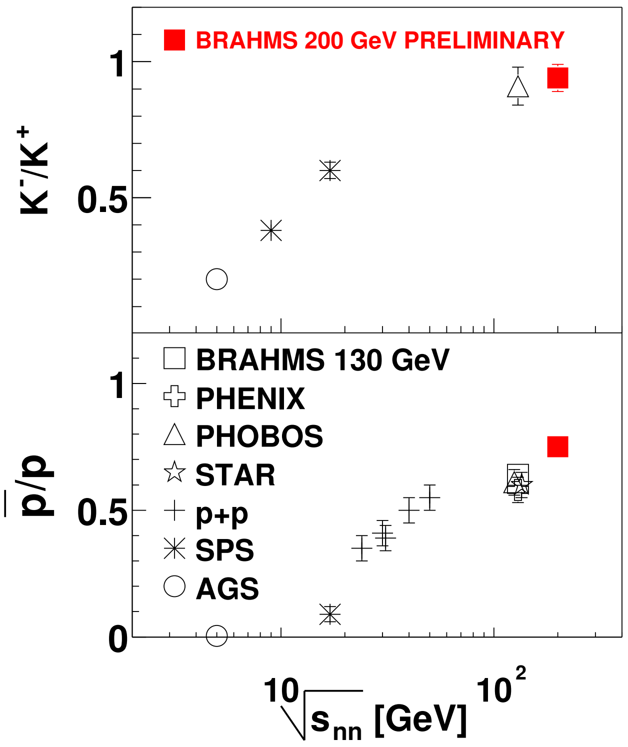

FIG. 10: Ratios as a function of $\sqrt{s_{NN}}$. Top: K^-/K^+; bottom: $\bar{p}/p$.

VI. CONCLUSION

In summary, the BRAHMS experiment has measured the ratio of negative to positive pions, kaons and protons at central and forward rapidities. It has been found that the pion ratio is close to unity as would be expected at these bombarding energies, where more than 5000 charged particles (predominantly pions) are produced per central collision. However, although the proton ratio at midrapidity increased from 0.64 for $\sqrt{s_{NN}} = 130$ GeV [10–12] to 0.75 for $\sqrt{s_{NN}} = 200$ GeV, it is still significantly below unity at $y = 0$ and decreases towards forward rapidities. This dependence on rapidity serves as an indicator of the balance between the baryon transport to midrapidities and anti-baryon and baryon pair production. The results suggest that there is still a significant contribution from participant baryons over the entire rapidity range and that the full transparency of the Bjorken model has not yet been reached. Nevertheless, reactions at the present energy evidence the highest antiparticle to particle ratios so far observed in nucleus-nucleus collisions.

[1] I. G. Bearden et al. (NA44), submitted to Phys. Rev. Lett. (2002), nucl-ex/0202019.

[2] F. Videbæk and O. Hansen, Phys. Rev. **C52**, 2684 (1995).

[3] J. D. Bjorken, Phys. Rev. **D27**, 140 (1983).

[4] J. Letessier and J. Rafelski, Int.J.Mod.Phys. **E9**, 107 (2000), nucl-th/0003014.

[5] M. Adamczyk et al. (BRAHMS), submitted to Nucl. Instrum. Meth. (2002).

[6] I. G. Bearden et al. (BRAHMS), Phys. Lett. **B523**, 227 (2001), nucl-ex/0108016.

[7] I. G. Bearden et al. (BRAHMS), submitted to Phys. Rev. Lett. (2001), nucl-ex/0112001.

[8] Z. Majka, *this proceeding*.

[9] X.-N. Wang and M. Gyulassy, Phys. Rev. **D44**, 3501 (1991).

[10] I. G. Bearden et al. (BRAHMS), Phys. Rev. Lett. **87**, 112305 (2001), nucl-ex/0106011.

[11] C. Adler et al. (STAR), Phys. Rev. Lett. **86**, 778 (2001).

[12] B. Back et al. (PHOBOS), Phys. Rev. Lett. **87**, 102301 (2001).